PHOTOVOLTAIC PROPERTIES OF CONJUGATED POLYMER/FULLERENE COMPOSITES ON LARGE AREA FLEXIBLE SUBSTRATES

Desta Gebeyehu[1*], F. Padinger[2], T. Fromherz[2], J.C. Hummelen[3], and N.S. Sariciftci[1]

[1]Christian Doppler Laboratory for Plastic Solar Cells, Physical Chemistry, Johannes, Kepler University of Linz, Altenbergerstr, 69, A-4040 Linz, Austria; [2]Quantum Solar Energy Linz, A-4040 Linz, Austria; [3]Stratingh Institute & Material Science Center, University of Groningen, Nijenborgh, 4, 9747 AG Groningen, The Netherlands

ABSTRACT. In this paper we present measurements of the photovoltaic response of bulk donor-acceptor heterojunction between the conjugated polymer, poly(3-octylthiophene), P3OT, (as a donor, D) and fullerene (methanofullerene), (as acceptor, A), deposited between indium tin oxide and aluminum electrodes. The innovation involves the substrate, which is a polymer foil instead of glass. These devices are based on ultrafast, reversible, metastable photoinduced electron transfer and charge separation. We also present the efficiency and stability studies on large area (6 cm x 6 cm) flexible plastic solar cells with monochromatic energy conversion efficiency (η_e) of about 1.5% and carrier collection efficiency of nearly 20%. Further more, we have investigated the surface network morphology of these films layers by atomic force microscope (AFM). The development of solar cells based on composites of organic conjugated semi-conducting polymers with fullerene derivatives can provide a new method in the exploitation of solar energy.

INTRODUCTION

The ability to dope conjugated polymers over the full range from insulating to conducting behavior resulted in fundamental research in this class of materials that combine the electronic and optical properties of semiconductors and metals with attractive mechanical properties as well as processing properties of polymers [1-4]. In this context solubility of processible films of conjugated polymers is the most crucial parameter since many methods to produced a well defined sample layer rely on solution processes (drop, spin and dip casting). Polymeric materials have technological advantages over conventional inorganic materials in the reduction of production costs by large scale production, the possibility to produce large area flexible devices and the tunability of the electronic bandgap by chemical synthesis. These properties represent major advances in the design of electronic devices.

Applications involving conjugated polymers include light emitting diodes, thin film transistors, sensors, and photovoltaic devices. In photovoltaic effect, electrons and holes are produced and are collected at the electrodes that sandwich the semiconductor. Unlike in inorganic semiconductors where free e/h$^+$ pairs are produced directly by light absorption, in organic semiconductors bound e/h$^+$ pairs (excitons) are created by irradiation. This exciton is ionized into an electron and hole by internal electric field or by applied potentials. It requires a proper choice of acceptors and donors to facilitate quick dissociation and fast collection of the charge carriers, which determine the efficiencies. Photoelectric energy conversion efficiencies for different organic solar cells, including small molecules as well as polymeric cells, are typically in the range of 1% [5-7]. The recently discovered photoinduced electron transfer in solutions and in solid state composites of semi-conducting, conjugated polymers

with fullerenes (C_{60}) has attracted considerable scientific and technological attention [8-9]. The possibility of utilizing this effect for photovoltaic energy conversion [10] has been demonstrated. With the addition of C_{60} in the conjugated polymer matrix, the primary photoexcitation of the conjugated polymer undergoes an ultrafast electron transfer, and it has been demonstrated that fullerene molecules may serve as efficient electron acceptors in polymeric cells [11].

Since the charge transfer takes place much faster than the radiative and/or non-radiative decay of photoexcitations, the quantum efficiency for charge separation in such D/A blends is near unity. Efficient polymeric photovoltaic solar cells have been made from phase separated composites of soluble conjugated polymers and C_{60} as well as from phase separated D/A polymer blends. Significant improvement of the relatively low collection efficiency of the D/A bilayer has been achieved by using phase-separated composite materials through control of the phase-separation into an interpenetrating networks of organic donors and acceptors sandwiched between two electrodes with different work functions. High efficiency conversion involves the formation of bicontinuous networks. The performance of such bulk heterojunction devices is remarkably enhanced compared to devices made from single components and bilayer devices. Carrier collection efficiency as high as 29% and monochromatic power conversion efficiency about 3% [12-17] have been reported. Studies of conjugated polymer/fullerene photovoltaic devices showed that the energy conversion efficiency is limited by the collection of the charges at the electrodes [12]. This inefficient transport of the charge carriers is explained by the limited mobility of both carriers, i.e. holes on the conjugated polymer as well as electrons on the fullerenes. The low mobility of the carriers is a consequence of the hoping conduction in the network. Solar cells with good performance based on the composite poly(2-methoxy-5-(3',7'-dimethyloctyloxy)-1,4-phenylene vinylene), MDMO-PPV and 1-(3-methoxycarbonyl)-propyl-1-phenyl-(6,6)C_{61}, PCBM (1:3 weight ratio) have been recently demonstrated [18-20]. Up to now, the laminated two layer polymeric photovoltaic diodes based on a cyano derivative of poly(p-phenylene vinylene), MEH-CN-PPV, as electron acceptor, and a derivative of polythiophene, POPT, as an electron donor, showed the highest efficiencies among this class. The resulting structures provide a short circuit photovoltaic quantum efficiency up to 29% at optimum wavelength, and an over all energy conversion efficiency of 4.8% at the peak wavelength [17].

Still now no systematic studies of the influence of oxygen atmosphere on the characteristics of conjugated polymer/fullerene photovoltaic devices are available. The limited stability of the conjugated polymer/fullerene photovoltaic devices under ambient conditions hinders the practical applications. Recent FTIR degradation studies on the composites showed rapid degradation of the conjugated polymer, MDMO-PPV compared to C_{60} or PCBM under oxygen and light [21]. In other words, conjugated polymers are known to be sensitive to photo-degradation in oxygen containing environment. Therefore, for practical applications, the stability especially of the polymer part of the mixture has to be improved and devices have to be protected. Since we found similar degradation results in P3OT/PCBM composite, we present here only results of controlled degradation experiments performed with the actual composite of P3OT/C_{60}.

Additional important parameter, determining the quality of thin films is the choice of the substrates. We studied here the I/V characteristics of the conjugated polymer/fullerene composites thin films on ITO polyester substrates with typical area of 6 cm by 6 cm and active areas of 4 times 40 mm^2.

In this study, we investigated polymeric devices based on the following composites: $P3OT/C_{60}$ (1:1 weight ratio), P3OT/(6,6)PCBM monoadduct or multiadduct (1:2 weight ratio), which is a derivative of C_{60} with improved solubility in xylene solutions at room conditions. Devices with fullerene and fullerene derivatives were characterized by I/V measurements under white light and monochromatic light as well as by wavelength dependent photocurrent measurements. From these data power efficiencies were calculated and compared to carrier collection efficiencies (incident photon to converted electron, IPCE). In the present study we have also shown the results of stability and controlled degradation experiments performed with the actual mixture used in plastic solar cells.

EXPERIMENTAL

The device configuration and device preparation for polymer photovoltaic cells (and photodetectors) were described in [9,11,6]. The photovoltaic devices produced here are composed of four layers as shown in Figure 1. First the PEDOT-PSS (poly(3,4-ethylenedioxythiophene)-poly(styrenesulfonate) (Baytron – Bayer AG) was spin coated (thickness approximately 100 nm) on transparent ITO (indium tin oxide)-coated polyester substrates with typical areas of 6 cm by 6 cm (surface resistance of 55 ohm/square). PEDOT is supported to prevent aggregation or separation between the two components of solar cell composite at these mixing ratios, which may lead to short contacts in our devices. After that the active bulk heterojunction layer was prepared by spin coating films of the composites: $P3OT/C_{60}$ (1:1 weight ratio), P3OT/(6,6)PCBM monoadduct or multiadduct (1:2 weight ratio) on the top of PEDOT-PSS layer. The P3OT was supplied from Neste. The preparation and characterization of PCBM, which is a derivative of C_{60} with improved solubility, is described in [22]. The PCBM multiadduct is a mixture of mono, bis, and tris adducts on the fullerene. After an additional drying step the low work function transparent aluminum top electrode was deposited by vacuum evaporation ($\sim 3 \times 10^{-6}$ mbar).

Cells have been produced under ambient conditions. No actions were taken to remove the residual oxygen from the cells, which maybe adsorbed on the surface during the production process. The degradation process was monitored by continuous I/V sweeps under ambient conditions.

To retard the degradation process of plastic solar cells, two attempts for the protection have been made. One of the attempts was lamination of the solar cells into special lamination foils. The lamination occurs inside the glove box to avoid oxygen inclusion inside the laminated solar cell. The lamination foils were glued to the cell by heat treatment and measured under ambient conditions. Another attempt was sealing with varnish inside a glove box under nitrogen flow.

A defocused Ar^+ laser beam at 488 nm provided the illumination and a calibrated Si Photodiode was utilized to measure light intensities. A Keithley SMU 2400 Source Meter was used for recording I/V curves when illuminating the cells through the ITO side, typically by averaging 80 measurements for one point. Optical absorption was obtained with a Hitachi spectrophotometer. Photocurrent excitation profiles were measured using a xenon arc lamp, spectrally resolved by a monochromator, at intensity of 1 mW/cm^2 at each wavelength in the range of between 400 nm and 700 nm.
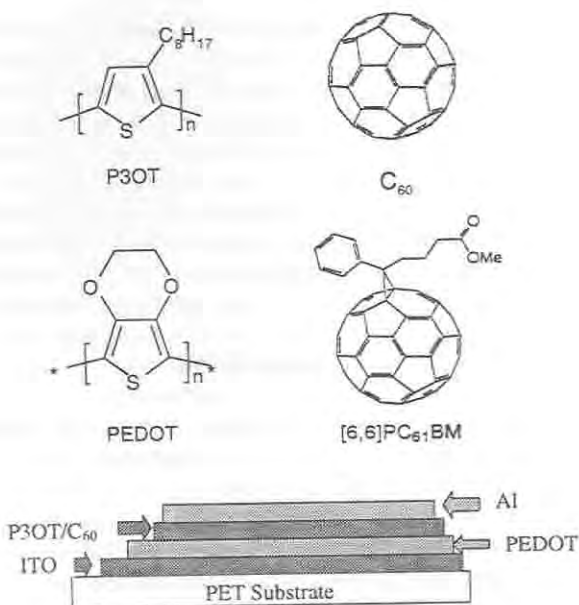
Figure 1. Schematic diagram of the device configuration and molecular structures of the materials used.

RESULTS AND DISCUSSION

All the solar cell devices produced here are in the sandwich geometry as mentioned abov between two metal electrodes with different work functions, ITO as anodes (as hole collecto and aluminum as cathode (as electron collector). Asymmetric work functions for th electrodes of organic interpenetrating network photovoltaic devices are necessary for significant reason. It has been shown that the charge transport between conjugated polyme and fullerenes is favorably tuned by electric field. The electric field due to the differe electrodes is the driving force to collect the charges at the electrodes. Without this there w be no selection principle for the holes to travel to the ITO and for the electrons to go to th aluminum electrodes

The thickness of semi-conducting organic films represents a crucial parameter for th performance in photovoltaic devices. The need to absorb most of the sunlight in solar ce requires a film thicker than 100 nm. On the other hand, thin layers enhance the intern electric field and improve the charge transport. In our work, the typical film thicknesses a around 150 nm. The quality and the homogeneity of the composite films strongly influen the efficiency of the solar cell. Inhomogeneous films with pin holes and large seri resisitivities lead to small fill factor (FF), lower rectification and decreased the open circ voltage (V_{oc}). In addition, it is clearly shown that the efficiency can be increased significant by decreasing the device thickness to an optimum value [19].

The calculation of overall energy conversion efficiency, η_c has been performed using the equation

$$\eta_c = (V_{oc}[V] * I_{sc}[A/cm^2] * FF)/P_{inc} [W/cm^2] \tag{1}$$

under different intensities, where V_{oc}, I_{sc}, FF and P_{inc} are the open circuit potential, short circuit current, filling factor and incident light power, respectively. We determine the value of the fill factor of the device, FF, by calculating of the maximum power rectangular area under the I/V curve in the 4th quadrant. Therefore, the filling factor is calculated by

$$FF = (V_{max} * I_{max})/ (V_{oc} * I_{sc}) \tag{2}$$

where V_{max} and I_{max} are maximum voltage and current of the intersection of the I/V curve with the maximum power rectangle, respectively. The photovoltaic external quantum efficiency (charge carrier per incident photon) or the spectrally resolved incident photon to electron converted efficiency IPCE (η_c) is calculated from the spectrally resolved short-circuit current [23],

$$\eta_c[\%] = 1240/\lambda[nm] * Isc[\mu A/cm^2]/I_{inc}[W/m^2] \tag{3}$$

where I_{inc} is the intensity of the incident light.

Figure 2 illustrates the I/V characteristics comparison of (a) ITO/PEDOT/P3OT:C_{60}/Al, (b) ITO/PEDOT/P3OT:PCBM monoadduct/Al and (c) ITO/PEDOT/P3OT:PCBM multiadduct/Al flexible large area plastic solar cells in a linear as well as in a logarithmic scale. We obtained comparably high values of the open circuit voltages for the devices made from P3OT/C_{60} and P3OT/PCBM multiadduct ($V_{op} \sim 630$ mV), as shown in Figure 2(a) and Figure 2(c). Even though the enhanced solubility of (6,6)PCBM monoadduct or multiadduct compared to C_{60} allows to achieve a high fullerene-polymer weight ratio, we obtain using PCBM monoadduct somewhat smaller short circuit current of 470 $\mu A/cm^2$ compared to short circuit current using C_{60}, $I_{sc} \sim 700 \mu A/cm^2$ (see Figure 2(a)). The I_{sc} of the P3OT/PCBM multiadduct device is almost a factor of two smaller than that of the P3OT/PCBM monoadduct device mentioned above. The typical FF values for our devices are between 0.27 and 0.33. From all devices presented in this paper the ones using P3OT/C_{60} show the highest rectification (~ 15 at ± 2 V) in the dark. In the forward direction at higher voltages show comparable dark and photocurrent values for ITO/PEDOT/P3OT:C_{60}/Al device. Based on an extremely fast excited electron transfer from light absorbing conducting polymers such as P3OT to embedded fullerene (C_{60}) molecules surprisingly thigh photocurrents are produced taking into account relatively low absorption coefficients of most polymers.

The typical data for these flexible large area plastic solar cells presented here are a V_{oc} of 550-650 mV and a FF = 0.3. For P3OT/C60 and P3OT/PCBM monoadduct devices an I_{sc} of 800 $\mu A/cm^2$ and 450 $\mu A/cm^2$ under monochromatic 10 mW/cm^2 illumination (argon laser at 488 nm) are recorded, respectively. The I_{sc} of the P3OT/PCBM monoadduct devices is almost a factor of two smaller than the P3OT/C_{60} devices mentioned above. Usually the value of the open circuit voltage for the bulk heterojunction devices is interpreted to arise from the work function difference of the two electrodes (Al = 4,3 eV; ITO = 4,7 eV) which would yield a V_{oc} of 400 mV or lower as found by other groups [23]. Therefore, the origin of an open circuit voltage as high as 650 mV is not fully understood.
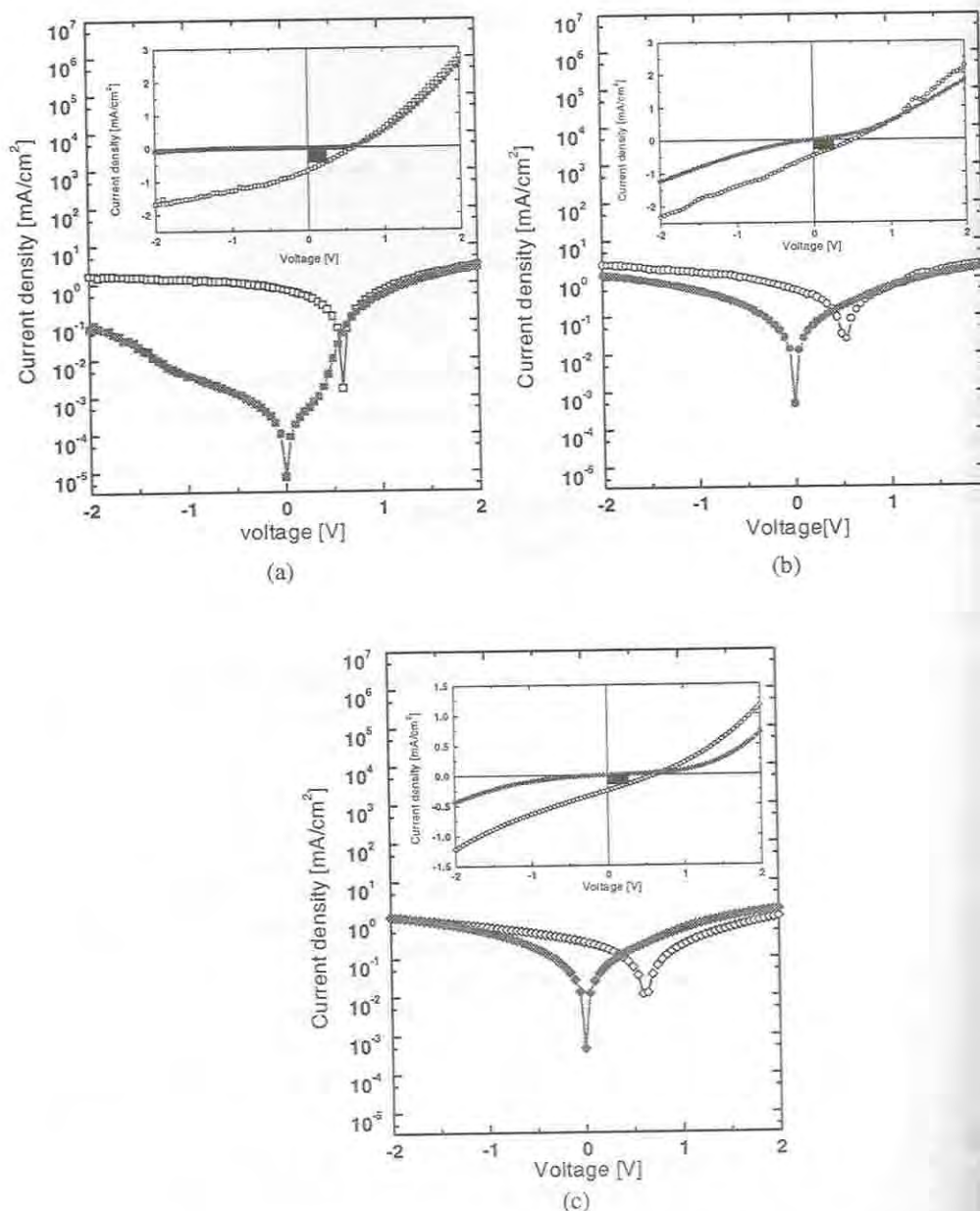
Figure 2. I/V characteristics comparison among (a) ITO/PEDOT/P3OT:C_{60}/Al (solid squares: dark, open squares: illuminated with white light, 6 mW/cm²), (b) ITO/PEDOT/P3OT:PCBM mono/Al (solid circles: dark, open circles: illuminated with white light, 6 mW/cm²) and (c) ITO/PEDOT/P3OT:PCBM multi/Al (solid diamond: dark, open diamond: illuminated with white light, 6 mW/cm²) of flexible large area plastic solar cells in a linear (inset) as well as the logarithmic scale.

The overall energy conversion efficiency, η_e, for the P3OT/C$_{60}$ and P3OT/PCBM monoadduct flexible plastic solar cells was calculated to be approximately 1.5% and 1% under monochromatic 10 mW/cm^2 illumination (488 nm), respectively. According to the experimental data, typical values for η_e are between 1% and 1.5%. It should be noted that in polymeric/organic devices the photoelectric conversion efficiency is, in many cases, strongly dependent on light intensity. Weak light usually gives high conversion efficiency. The maximum value of the electron to photon conversion efficiency of a P3OT/C$_{60}$ solar cell is found to be about 20% at 488 nm, which is comparable to the earlier report [24]. On the other hand for a P3OT/PCBM monoadduct flexible large area plastic solar cell, we achieved the short circuit photovoltaic external quantum efficiency ($\eta_e[\%]$) of about 11% under an argon laser at 488 nm with 10 mW/cm^2 and a I$_{sc}$ of around 450 µA/cm^2.

Figure 3 shows a comparison between the spectrally resolved I$_{sc}$ (solid circles) plotted at the right axis and the optical density (open circles) at the left axis of a P3OT/ C$_{60}$ flexible large area plastic solar cell. One can see very clearly, that the two curves have the same onset and spectrally resolved maxima separated by only 18 nm. The absence of matching of optical absorption and photocurrent in the range of 400-500 nm is may be due to the material parameter or due to the film production process.
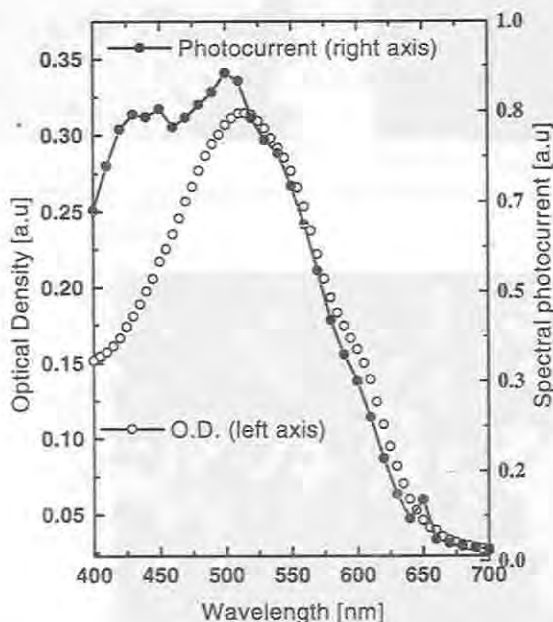

Figure 3.   Spectrally resolved I$_{sc}$ (solid circles) of a P3OT/C$_{60}$ flexible large area plastic solar cell (right axis), optical absorption (open circles) is plotted for comparison (left axis).

We expect further improvements in device efficiencies by optimizing the network morphology of the composite materials. Therefore, atomic force microscope (AFM) was used to study the surface morphological structure of the composite films. Figure 4 illustrates an AFM comparison of the (a) P3OT/C$_{60}$, (b) P3OT/PCBM monoadduct and (c) P3OT/PCBM

multiadduct composite films. The pictures were taken directly from the devices after the measurement. As we see from the figure, P3OT/C_{60} composite films show very homogeneous films in the sub-μm scale. In contrast, the P3OT/PCBM monoadduct blend films show strong phase separation on a horizontal scale of several μm. Evidence of pinholes with depths of ~30 nm is also seen in the P3OT/PCBM films. On the other hand, P3OT/PCBM multiadduct composite films show very flat homogeneous film with pinholes about 50 nm depths.
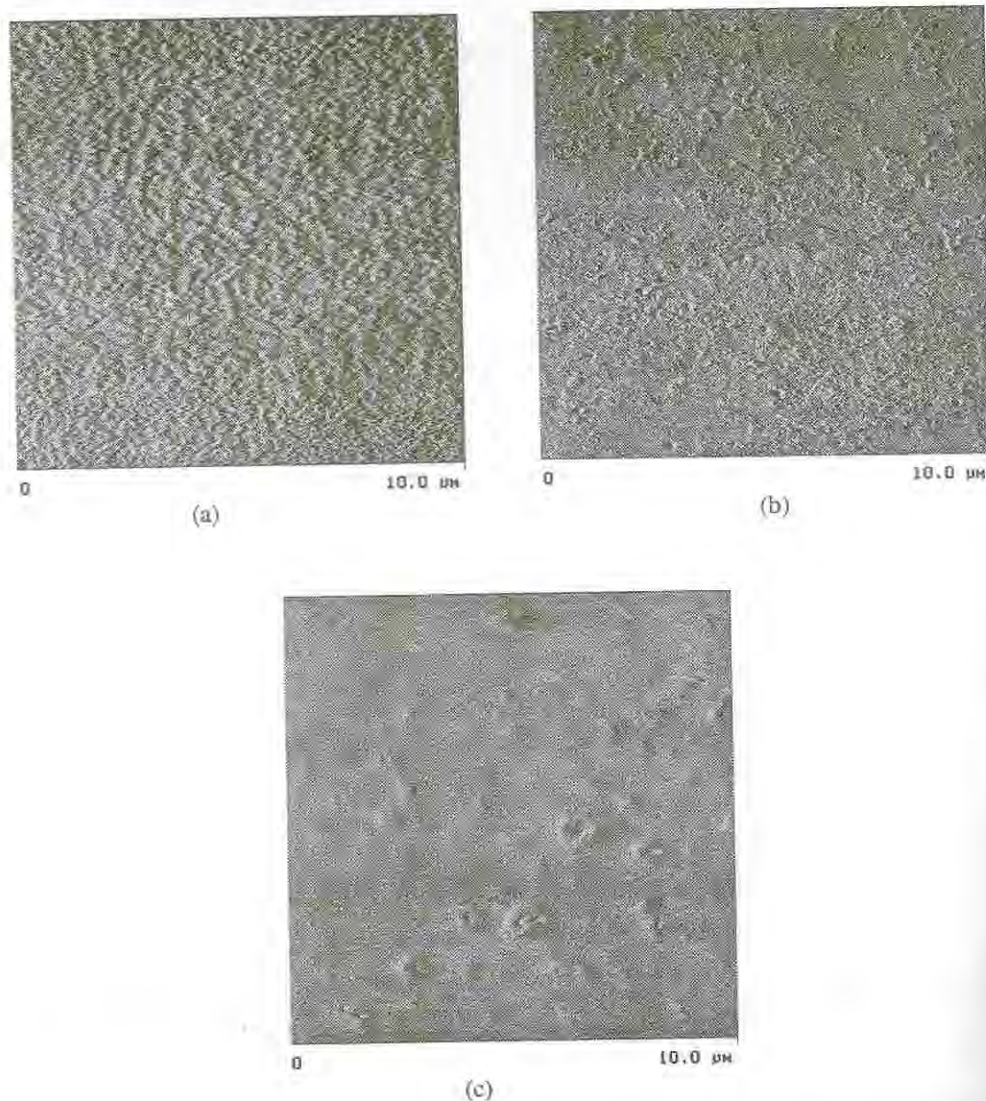
0   10.0 μM
(a)

0   10.0 μM
(b)

0   10.0 μM
(c)

Figure 4.   AFM comparison of the (a) P3OT/C_{60} (1:1 weight ratio), (b) P3OT/PCBM monoadduct (1:2 weight ratio) and (c) P3OT/PCBM multiadduct (1:2 weight ratio) composite films.

For practical applications, the stability of plastic solar cells under ambient conditions is one of the most important issues. Therefore, a quick and reliable testing procedure for photodegradation effects in oxygen containing environment is necessary. In [21] the results showed that high degradation rate found for polymeric part of the solar cell mixture under the influence of light and oxygen is significantly decreased when the polymer is mixed with fullerenes (as used in plastic solar cells). Obviously, the fast charge transfer from the polymer to C_{60} after excitation accompanied with the formation of positively charged polarons on the chain decreases strongly the reactivity of the polymer against oxygen. Therefore, for practical applications, the stability especially of the polymeric part of the composite has to be improved and devices have to be effectively protected in order to achieve high life times. Figure 5 shows the degradation of a P3OT/C_{60} unprotected solar cell monitored by the changes in the V_{oc} as a function of time under oxygen and white light source with 8 mW/cm². After approximately 60 hours V_{oc} decreases to half of its original value. Figure 6 illustrates the degradations of I_{sc} unprotected solar cell versus time under white light source 35 mW/cm² and oxygen containing environment. As can be seen from measured degradation time, the curve is fitted to an exponential decay and a lifetime of 70 minutes. To retard the degradation process of plastic solar cells, some attempts for the protection have been made. The long term stability of protected plastic solar cells is monitored by V_{oc} and I_{sc} measurements under ambient room conditions. In Figure 7, the V_{oc} and the I_{sc} versus shelf lifetime of protected plastic solar cells with varnish are shown. Encapsulation of plastic solar cells increases the shelf lifetime over 100 days. The initial decrease of V_{oc} and I_{sc} could be due to the residual oxygen during the cell production process.
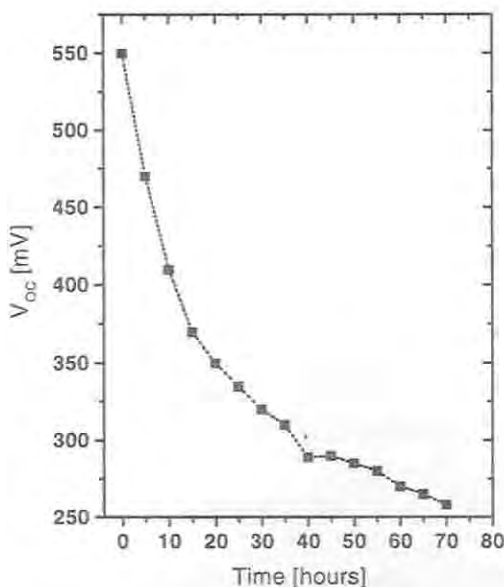

Figure 5.   Degradation of V_{oc} of a P3OT/C_{60} unprotected solar cell versus time under bright light and oxygen influence.
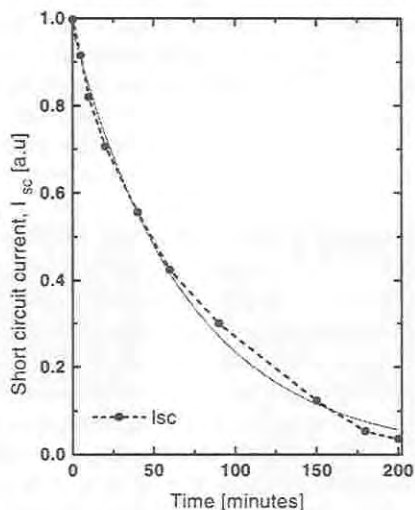
Figure 6.   Short circuit current, I_{sc}, degradation *vs.* time of unprotected P3OT/C$_{60}$ plastic solar cell. The curve is fitted to an exponential decay.
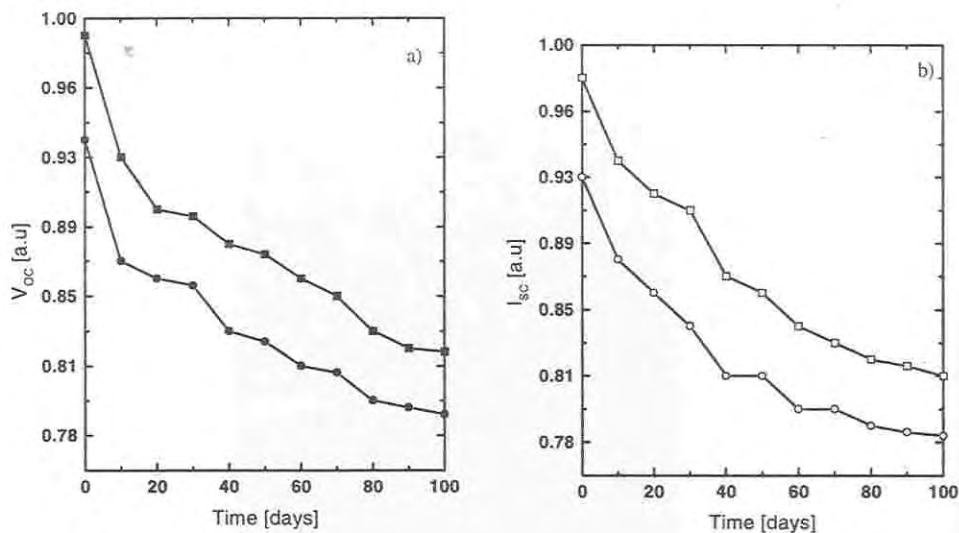

Figure 7.   Comparison of (a) V_{oc} (solid squares and solid circles) and (b) I_{sc} (open squares and open circles) *vs.* shelf lifetime of two different strips of a P3OT/C$_{60}$ protected plastic solar cells.

CONCLUSION

Photovoltaic cells, based on composites of processable conjugated polymers and fullerene derivatives, are more and more considered as potentially promising devices for future solar energy production. At present, the efficiency of such plastic PV cells is limited, the devices only produce current when a relatively thin layer is used. Although a lot of fundamental studies have been performed in polymer/C_{60} composite, there is still fundamental lack of understanding of the so-called interconnected networks formed by the C_{60} molecules. The photovoltaic conversion efficiency of plastic solar cells based on conjugated polymer-fullerene bulk heterojunction is limited by the carrier collection efficiency (i.e. the separated charges must be collected with the minimum losses) and by charge transport. For photovoltaic devices fabricated from several blends of P3OT/C_{60} and its derivatives (PCBM mono and multiadducts), the highest short circuit current were obtained with blend of P3OT and C_{60} (1:1 weight ratio). In this work, the highest realized photovoltaic devices show monochromatic power efficiency, η_c of 1.5% and an IPCE of about 20%. On the other hand for the best flexible plastic solar cells realized here, an overall light to electric energy conversion efficiencies of about 0.4% - 0.6% are calculated in simulated solar light (AM1.5). We expect further improvements in device efficiencies by optimizing the composite composition, the network morphology and the charge transport properties of the individual components.

Unprotected plastic solar cells show current and voltage degradation under oxygen environment and light. Within the actual mixture used in plastic solar cells, the degradation rate of open circuit voltage, V_{oc} is much slower compared to the short circuit current, I_{sc}. This is proposed to arise from the increased trapping of the charge carriers due to degradation induced defects. Laminating and sealing the solar cells decreases the degradation rate, but it does not completely prevent degradation. Compared to unprotected plastic solar cells, cells protected against the influence of oxygen and humidity have increased shelf lifetime by at least a factor of 100. Our results indicate an increase of the overall serial resistivity by degradation. Large scale processing of solar cells from conjugated polymer/fullerene devices may become relevant for photoelectric energy conversion. A very important parameter for industrial applications is the lifetime of the devices. Stabilization of these composites is realized by the rigorous exclusion of oxygen.

ACKNOWLEDGEMENTS

REFERENCES

1. Sariciftci, N.S.; Heeger, A.J. in *Handbook of Organic Conductive Molecules and Polymers*, Vol. 1, Halwa, H.S. (Ed.); Wiley: New York; 1997; pp 413-455.
2. Kanicki, T.J. in *Handbook of Conducting Polymers*, Skotheim, T.A. (Ed.); Dekker: New York; 1986; pp 543-660.
3. Bredas, J.L.; Silbey, R. *Conjugated Polymers*, Kluwer Academic: Dodrecht; 1991.

4. Salaneck, W.R.; Clark, D.T.; Samuelsen, E.J. *Science and Application of Conductir Polymers*, Hilger: Bristol; 1991.
5. Tang, C.W. *Appl. Phys. Lett.* **1986**, 48, 183.
6. Yu, G.; Gao, J.; Hummelen, J.C.; Wundl, F.; Heeger, A.J. *Science* **1995**, 270, 1789.
7. Rostalski, J.; Meissner, D. *Proceedings of European Conference on Organic Solar Cell ECOS*, 1998, Cadarache, France; *Solar Energy Materials and Solar Cells* **2000**, 61, 87.
8. Sariciftci, N.S.; Smilowitz, L.; Heeger, A.J.; Wudl, F. *Science* **1992**, 258, 1474.
9. Sariciftci, N.S.; Heeger, A.J. in *Handbook of Organic Conductive Molecules ar Polymers* Vol.1, Halwa, H.S. (Ed.); Wiley: New York; 1997; pp 437-440.
10. Sarciftci, N.S.; Braun, D.; Zhang, C.; Srdanov, V.; Heeger, A.J.; Stucky, G.; Wudl, *Appl. Phys. Lett.* **1992**, 62, 585; Morita, S.; Zakhaidov, A.A.; Yoshino, K. *Sol. Sta Commun.* **1992**, 82, 249.
11. Sariciftci, N.S. *J. Prog. Quant. Electr.* **1995**, 19, 131.
12. Gao, J.; Wang, H.; Hide, F. *Synthetic. Met.* **1997**, 84, 979.
13. Veenstra, S.C.; Malliaras, G.G.; Brouwer, H.J.; Esselink, F.J.; Krasnikov, V.V.; v Hutten, P.F.; Wildeman, J.; Jonkman, H.T.; Sawatzky, G.A.; Hadziioannou, G. *Synthet Met.* **1997**, 84, 971.
14. Yoshino, K.; Tada, K.; Fujii, A.; Conwell, E.M.; Zakhidov, A.A. *IEEE Trans Electr Dev.* **1997**, 44, 1315.
15. Halls, J.J.M.; Walsh, C.A.; Greenham, N.C.; Marseglia, E.A.; Friend, R.H.; Moratti, S.(Holmes, A.B. *Nature* **1995**, 376, 498.
16. Yu, G.; Heeger, A.J. *J. Appl. Phys.* **1995**, 78, 4510.
17. Granström, M.; Petritsch, K. Arias, A.C.; Lux, A.; Andersson, M.R.; Friend, R.H. *Natu* **1998**, 395, 257.
18. Brabec, C.J.; Padinger, F.; Hummelen, J.C.; Janssen, R.A.J.; Sariciftci, N.S. *Synthe Met.* **1999**, 102, 861.
19. Fromherz, T.; Padinger, F.; Gebeyehu, D.; Brabec, C.; Hummelen, J.C.; Sariciftci, N *Proc. ECOS*, 1998, Cadarache, France; *Solar Energy Materials and Solar Cells*, in press
20. Padinger, F.; Fromherz, T.; Brabec, C.; Gebeyehu, D.; Hummelen, J.C.; Sariciftci, N *Proc. QUANTSOL*, 1999, Wildhaus, Switzerland.
21. Neugebauer, H.; Brabec, C.J.; Sariciftci, N.S. *Synthetic. Met.* **1999**, 102, 1002.
22. Hummelen, J.C.; Wright, B.W.; Lepec, F.; Wudl, F. *J. Org. Chem.* **1995**, 60, 532.
23. Roman, L.R.; Anderson, M.R.; Yohannes, T.; Inganäs, O. *Adv. Mater.* **1997**, 9, 11(Yoshino, K.; Tada, K.; Hirohata, M.; Kajii, H.; Hironaka, Y.; Tada, N.; Kaneuchi, Yoshida, M.; Fijii, A.; Hamagchi, M.; Araki, H.; Kawai, T.; Ozaki, M.; Ohmri, Y.; Onoc M.; Zakhidov, A.A. *Synthetic. Met.* **1997**, 84, 477.
24. Gebeyehu, D.; Padinger, F.; Brabec, C.J.; Fromherz, T.; Hummelen, J.C.; Sariciftci, N *Intern. J. Photoenergy*, **1999**, 1, 89.